Bioresource Technology 294 (2019) 122185

Contents lists available at ScienceDirect

Bioresource Technology

journal homepage: www.elsevier.com/locate/biortech

Nitrate stimulation of N-Methylpyrrolidone biodegradation by *Paracoccus pantotrophus*: Metabolite mechanism and Genomic characterization

Jing Wang[a], Xiaolin Liu[a], Xinbai Jiang[a], Libin Zhang[a,*], Cheng Hou[a], Guanyong Su[a], Lianjun Wang[a], Yang Mu[b], Jinyou Shen[a,*]

[a] Jiangsu Key Laboratory of Chemical Pollution Control and Resources Reuse, School of Environmental and Biological Engineering, Nanjing University of Science and Technology, Nanjing 210094, China
[b] CAS Key Laboratory of Urban Pollutant Conversion, Department of Applied Chemistry, University of Science and Technology of China, Hefei 230026, China

GRAPHICAL ABSTRACT

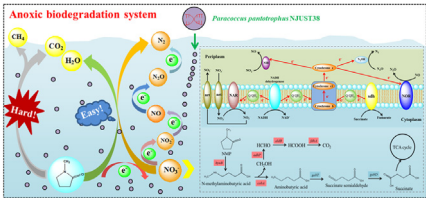

ARTICLE INFO

Keywords:
N-Methylpyrrolidone
Biodegradation
Denitrification
Paracoccus
Functional genes

ABSTRACT

Due to the toxicological nature of N-methylpyrrolidone (NMP), the conventional anaerobic bioprocess is quite ineffective for NMP removal from wastewater. In order to achieve effective NMP biodegradation under anoxic condition, *Paracoccus pantotrophus* NJUST38 was isolated for the first time. The supplementation of nitrate into anoxic system resulted in complete removal of 5 mM NMP by NJUST38 within 11 h compared to 24% in the anaerobic control system in the absence of nitrate. Genome characterization revealed that NMP biodegradation catalyzed by several key enzymes/genes, including N-methylhydantoin amidohydrolase (*hyuB*), methyltransferase (*cobA*), 4-aminobutyrate-2-oxoglutarate transaminase (*gabT*), succinate-semialdehyde dehydrogenase (*gabD*) and so on. NMP biodegradation pathway was proposed based on several intermediates, where NMP was biodegraded mainly for providing electrons and reducing power to support microbial denitrification through tricarboxylic acid (TCA) cycle. The proposed mechanism should aid our mechanistic understanding of NMP biodegradation by *Paracoccus pantotrophus* and the development of sustainable bioremediation strategies.

1. Introduction

N-Methylpyrrolidone (NMP) is a typical organic polar solvent that is characterized by its excellent water-miscibility, low volatility, high polarity and noncorrosive properties, and it is extensively used in the manufacture of adhesives, paints, fuels, and pharmaceuticals (Zolfaghari et al., 2011; Liang et al., 2018). Due to its high water solubility, NMP is prone to access the environment via release in wastewater. As a consequence, the observed NMP concentration in industrial wastewater is often higher than 1000 mg L^{-1} (Campbell and Striebig 1999; Loh et al., 2018). It was estimated that more than 2400 tons of NMP is discharged or transferred into the environment annually via the discharge of wastewater (Cai et al., 2014). Considering the inherent teratogenicity and toxicity of NMP, 1 mg L^{-1} is the recommended occupational exposure by the Japanese Society for Occupational Health (Zolfaghari et al., 2011). Therefore, the development of

* Corresponding authors.
E-mail addresses: lbzhang@njust.edu.cn (L. Zhang), shenjinyou@mail.njust.edu.cn (J. Shen).

https://doi.org/10.1016/j.biortech.2019.122185
Received 24 August 2019; Received in revised form 19 September 2019; Accepted 20 September 2019
Available online 24 September 2019
0960-8524/

effective approaches to solve the potential threat of NMP contamination is rather urgent.

Various physico-chemical methods, such as photodegradation (Zolfaghari et al., 2011), ozone oxidation (Campbell and Striebig, 1999) and membrane separation (Loh et al., 2018), were proposed for the removal of NMP from contaminated wastewater. However, the application of multifarious physico-chemical methods is limited in practical applications due to the challenges of high cost, high energy consumption and serious secondary pollution (Campbell and Striebig 1999; Wang et al., 2010; Yau et al., 2015). Biological processes, which were often consist of anaerobic and aerobic units (A-O process), are a promising alternative to deal with wastewater containing various recalcitrant pollutants due to its cost effectiveness and environmental friendliness (Yun et al., 2017; Lee et al., 2001; Jiang et al., 2018; Wu et al., 2019). However, the conventional A-O process is often limited by the lack of specific functional degrading species due to the toxicity of NMP. Several aerobic strains are capable of utilizing NMP as the sole carbon and nitrogen source, including genera *Paracoccus* (Loh et al., 2018; Cai et al., 2014), *Alicycliphilus* (Solis-Gonzalez, et al., 2018), *Pseudomonas*, *Acinetobacter* and *Rhodococcus* (Krizek et al., 2015). Solis-Gonzalez et al. (2018) identified a six-gene cluster (*nmpABCDEF*) from *Alicycliphilus* sp. Strain BQ1 that encoded enzymes involved in NMP biodegradation. The *nmpA* and *nmpB* genes encoded an N-methylhydantoin amidohydrolase that transformed NMP to γ-N-methylaminobutyric acid, which is metabolized by an amino acid oxidase encoded by *nmpC*, to produce γ-aminobutyric acid via demethylation or succinate semialdehyde via deamination. Succinate semialdehyde may be transformed by a succinate semialdehyde dehydrogenase to succinate, which finally enters the Krebs cycle. Cai et al. (2014) proposed NMP oxidization to N-methylsuccinimide via *Paracoccus* sp. NMD-4, followed by cleavage of the two C-N bonds to form succinaldehyde, which may be oxidized to succinic acid for entry into the Krebs cycle. However, to the best of our knowledge, strains capable of biodegrading NMP under anaerobic or anoxic conditions were never reported.

Recently, substantial promotion of biodegradation efficiency towards various recalcitrant contaminants in anoxic systems in the presence of various alternative electron acceptors, such as nitrate (Carvajal et al., 2018; Mahdavianpour et al., 2018), sulfate (Li et al., 2018) or an electrode (Yan et al., 2017; Chen et al., 2019a), was widely revealed. Wang et al. (2018b) found that the anoxic biodegradation of an emerging organic contaminant, namely, triclosan, was achieved in the presence of nitrate, and the toxicity was remarkably reduced simultaneously. Zhang et al. (2016) indicated that dimethyl phthalate was effectively removed during anoxic incubation, and the removal performance was obviously superior to an anaerobic control system without nitrate. Our previous studies achieved enhanced pyridine biodegradation in the anoxic biodegradation systems supplemented with nitrate (Shen et al., 2015; Hou et al., 2018). These successful cases suggest that enhanced anoxic biodegradation of NMP by available electron acceptors, such as nitrate, is a promising alternative. It was well known that microbial denitrification needs to consume electrons to accomplish the reduction of NO_3^- to NO_2^-, NO, N_2O, and finally to N_2 (Wan et al., 2016). Su et al. (2019) indicated that the electron carrier namely nicotinamide adenine dinucleotide (NADH), which is produced through organic matters degradation, is the direct electron donor for these sequential reduction reactions (Chen et al. 2019b). Therefore, electrons transport system (ETS) including electron production, transport and consumption, can play a vital role in both denitrification and microbial metabolism. To develop an effective anoxic biodegradation strategy for the treatment of NMP-containing wastewater, it is quite essential to isolate microbial species that are capable of degrading NMP under anoxic conditions. Further investigation should provide key insights into anoxic NMP biodegradation, including biodegradation mechanisms, functional enzymes/genes and electron transport pathway dominating NMP biodegradation and denitrification.

With these considerations, the present study investigated the feasibility of NMP biodegradation under anoxic conditions with the additional of electron acceptor (i.e., nitrate). For the first time, a strain capable of degrading NMP under anoxic conditions was isolated from activated sludge acclimatized by NMP. To verify the mechanism of the observed bioprocess, the genome characteristics of this NMP-degrading strain was analyzed by genome sequencing, while the gene expression level was explored through transcriptome analysis. Finally, the key enzymatic activities, electron transport system (ETS) activity and NADH content, were investigated to further verify proposed NMP metabolic mechanism.

2. Materials and methods

2.1. Culture enrichment and strain isolation

Before the isolation of NMP-degrading stains, activated sludge from a biological contact oxidation tank treating NMP-containing wastewater was first enriched in mineral salts medium (MSM). MSM was composed of the following chemicals: 7 mM phosphate buffer (KH_2PO_4 and Na_2HPO_4, pH = 7.0), 0.2 g L^{-1} $MgSO_4{\cdot}7H_2O$, 0.05 g L^{-1} $CaCl_2$ and 10 mL L^{-1} trace element solution (Wang et al., 2018a). $NaNO_3$ and NMP were added at the desired concentrations. Before use, all media were purged with helium gas for 20 min to remove oxygen, followed by autoclaving at 121 °C for 30 min. The enrichment was performed in 120-mL serum bottles on a rotary shaker at 30 °C and 180 rpm under anoxic conditions. During the enrichment, NMP and $NaNO_3$ were added to the MSM at 3.0 mM and 6.5 mM, respectively. After approximately 60 days of enrichment, the enriched culture was serially diluted using 7 mM phosphate buffer (pH = 7.0) and spread onto presterilized MSM agar plates containing 5.0 mM NMP and 10.8 mM $NaNO_3$. Plates were incubated for 48 h, and morphologically distinct colonies were selected and transferred individually for further purification. A bacterium named after NJUST38 most effectively biodegraded NMP, and it was isolated successfully.

2.2. NMP biodegradation assays

Before NMP biodegradation experiments, a bacterial suspension of NJUST38 was prepared as the inocula. NJUST38 was inoculated into LB medium supplemented with 5 mM NMP and incubated on a rotary shaker at 180 rpm and 30 °C for 48 h before the biomass was harvested via centrifugation at 6000 rpm for 10 min. The deposit was resuspended and rinsed three times with 100 mL sterilized MSM to remove the nutritional composition in the LB medium. The bacterial deposit was diluted with sterilized MSM to an optical density of approximately 2.0 at a wavelength of 600 nm (OD_{600}). The obtained bacterial suspension was used as the inocula in the subsequent biodegradation assays at an inoculation size of 5% (v/v).

The NMP biodegradation performance by NJUST38 was evaluated using a series of 120-mL serum bottles as batch reactors. 100 mL sterilized MSM containing 5.0 mM NMP and 10.8 mM $NaNO_3$ was added to each reactor (i.e., anoxic condition). Each serum bottle was sealed with butyl-rubber stopper and crimped with aluminum cap. All serum bottles were purged with helium gas for 20 min to remove oxygen, followed by autoclaving at 121 °C for 30 min. Thereafter, 5 mL bacterial suspension was inoculated in serum bottle and incubated on a rotary shaker at 180 rpm and 30 °C. The anaerobic control test was carried out following the same procedure as describe above except for the absence of nitrate. The abiotic control test was performed following the same procedure as anaerobic control test except for the absence of the bacterial suspension. All of the tests were conducted for three replicates, with the independent analysis data averaged and the standard deviation calculated.

2.3. Analytic methods

NMP was identified and quantified using high-performance liquid chromatography (HPLC, DAD-3000, Thermo Scientific, USA). All water samples were filtered through 0.22-μm syringe filters, and 10 μL filter liquor was injected into the HPLC. HPLC analysis was performed using a C_{18} column (5 μm, 4.6 × 250 mm) at a column temperature of 30 °C and UV–vis wavelength of 214 nm. The mobile phase was 20% methanol and 80% ultrapure water (v/v), which was pumped at the flow rate of 1.0 mL min^{-1}. NMP biodegradation intermediates were identified using liquid chromatography-mass spectrometry (HPLC/MS) (Wang et al., 2018a). NO_3^--N, NO_2^--N and NH_4^+-N were measured according to Hou et al (2018). Total organic carbon (TOC) concentration was determined on a vario TOC analyzer (Germany Elementar).

NO concentration was monitored using a commercial gas analyzer (VARIO PLUS, MRU, Germany) (Ren et al., 2011). N_2O was determined using a gas chromatograph (GC, 7890A, Agilent, USA) with an electron capture detector (Li et al., 2017). N_2 was measured using GC (SP-6890, Lunan, China) with a thermal conductivity detector (Zhao et al., 2012). Cell morphology was examined using a cold field emission scanning electron microscopy (SEM, S-4800, Hitachi, Japan). The bacterial growth was monitored via the recording of variations in OD_{600} using a UV–vis spectrophotometer (Lambda25, Perkim Elmer, USA). A fluorescence excitation-emission matrix (EEM) was constructed in accordance with Wu et al (2018). Toxicity reduction during NMP biodegradation was evaluated according to Xu et al (2018).

2.4. Bacterial identification and genome sequencing

Bacterial identification was performed using 16S rRNA gene sequence combined with biochemical testing and bacterial morphology. The colony of NJUST38 appeared light yellow with a smooth and wet surface. The physiological and biochemical characteristics demonstrated that NJUST38 was Gram negative, oxidase and nitrate reductase positive. NJUST38 was spherical with a diameter of 0.48–0.69 μm. Sequences of NJUST38 were amplified with primers 1492R (5′-GGTT ACCTTGTTACGACTT-3′) and 27F (5′-AGTTTGATCMTGGCTCAG-3′). The 16S rRNA gene sequence of NJUST38 was submitted to NCBI for BLAST analysis, and the sequence was deposited in the GenBank database under accession NO. MH729824. The phylogenetic tree was constructed using neighbor-joining algorithms of MEGA5.1. The results revealed that NJUST38 was closely related to *Paracoccus pantotrophus* strain B21-3 (KT715779.1) and *Paracoccus pantotrophus* strain JCM6892 (AB598745.1). Therefore, NJUST38 was determined as a member of the family *Paracoccus pantotrophus*.

The genome of NJUST38 was sequenced using Illumina HiSeq PE150 in Novogene Bioinformatics Technology Co., Ltd. (Beijing, China). The *de novo* assembly for the sequences was performed using SOAPdenovo into scaffolds. Gene prediction and functional annotations were performed using Subsystem Technology server and NCBI's Prokaryotic Genome Annotation Pipeline.

2.5. Transcriptome sequencing, gene annotation and expression

Total two samples were collected from anaerobic system (labeled as Aa1.1 and Aa1.2 in Aa1 group) and four samples were collected from anoxic system (labeled as Ao1.1 and Ao1.2 in Ao1 group; Ao2.1 and Ao2.2 in Ao2 group) for RNA extraction. Sequencing libraries were generated using the NEBNext Ultra Directional RNA Library Prep Kit for Illumina (NEB, Ipswich, MA, USA). Paired-end sequencing was performed on an Illumina Hiseq 2500 platform. Before proceeding with the assembly, the clean reads were filtered from the raw reads by quality control and removal of the reads with (1) sequence adapters, (2) more than 10% "N" bases, and (3) more than 50% Q_{phred} (Phred score) ≤ 20 bases.

The gene expression level was calculated using the FPKM method (Wang et al., 2018c). The differential gene expressions (DGEs) were analyzed using DESeq software (version 1.10.1). Gene expression dynamics was measured by the log2.FoldChange (up-regulated: log2.FoldChange ≥ 0; significantly up-regulated: log2.FoldChange ≥ 2). The Gene Ontology (GO) and Kyoto Encyclopedia of Genes and Genomes (KEGG) analyses were performed according to Young et al. (2010).

2.6. Key enzyme activity, NADH content and electron transport system activity

The activities of N-methylhydantoin amidohydrolase (NMA), nitrate reductase (NAR), nitrite reductase (NIR), nitric oxide reductase (NOR) and nitrous oxide reductase (N_2OR) as well as NADH content were determined using the corresponding commercial kits (JingKang biological, China). The electron transport system (ETS) activity was determined according to Tian et al. (2017). Briefly, 0.5 mL bacteria culture was added into a 10.0 mL tube, followed by the addition of 2.0 mL Tris-HCl (pH = 8.4) and 1.0 mL 0.2% 2-(p-iodophenyl)-3-(p-nitrophenyl)-5-phenyltetrazolium chloride (INT). After the mixture was incubated at 35 °C for 30 min, 1.0 mL of formaldehyde (37%) was added to terminate the reaction and the mixture was centrifuged at 10,000 *g* for 2 min to collect the cells. Afterward, 5.0 mL methanol was added to extract INF. Finally, the mixture was centrifuged, and the supernatant was immediately measured spectrophotometrically at 485 nm against a solvent blank.

3. Results and discussion

3.1. NMP biodegradation, nitrogen conversion and toxicity reduction

In the biodegradation system inoculated with NJUST38, NMP removal performance showed significant differences with or without NO_3^-. As indicated in Fig. 1a, 5.0 mM NMP was completely removed within incubation time as short as 11.0 h with the supplementation of 10.8 mM NO_3^-. However, NMP concentration gradually decreased to 3.7 ± 0.1 mM within 8.5 h in the absence of nitrate, and then declined slowly until the end of the incubation period. TOC removal showed a similar profile (Fig. 1b). With the supplementation of 10.8 mM NO_3^-, TOC concentration decreased significantly from 309.6 ± 10.0 mg L^{-1} to 66.0 ± 6.0 mg L^{-1} within incubation time as short as 11.0 h, whereas TOC only decreased to 261.1 ± 11.5 mg L^{-1} within 11.0 h in the absence of NO_3^-. An obvious increase in OD_{600} value was accompanied by the removal of NMP and TOC. However, OD_{600} values in the presence of NO_3^- (i.e., anoxic condition) were always higher than those in the absence of NO_3^- (i.e., anaerobic condition), indicating the stimulating role of NO_3^- towards biomass growth. In the abiotic control experiment, NMP and TOC concentrations maintained constant values during the entire incubation period.

In the denitrification process using various organic compounds as electron donors, NO_3^- is reduced to N_2, with NO_2^-, NO and N_2O found as the major intermediates (Wan et al., 2016). After the inoculation of NJUST38, NO_3^--N content decreased obviously from 10.8 mmol L^{-1} to 0.2 ± 0.1 mmol L^{-1} after 11.0 h, while NO_2^--N content significantly increased to 4.2 ± 0.4 mmol L^{-1} at 7.5 h, but then decreased to 0.3 ± 0.1 mmol L^{-1} at 11.0 h (Fig. 1c). N_2 production was observed after incubation for 2.0 h and N_2-N content increased to 10.4 ± 0.9 mmol L^{-1} after incubation for 11.0 h, indicating the dominance of N_2 as denitrification product. However, NO-N and N_2O-N content were always below 0.002 ± 0.001 mmol L^{-1} and 0.008 ± 0.002 mmol L^{-1} at any incubation time, indicating the high activity of NOR and N_2OR. It was well established that nitrogen in various organic-N compounds is generally transformed into NH_4^+-N during biodegradation process (Jiang et al., 2018). However, NH_4^+-N concentration during the entire biodegradation process was always undetectable. Notably, the total inorganic-N content obviously increased from the initial 10.8 mmol L^{-1} to 12.5 ± 0.9 mmol L^{-1} after

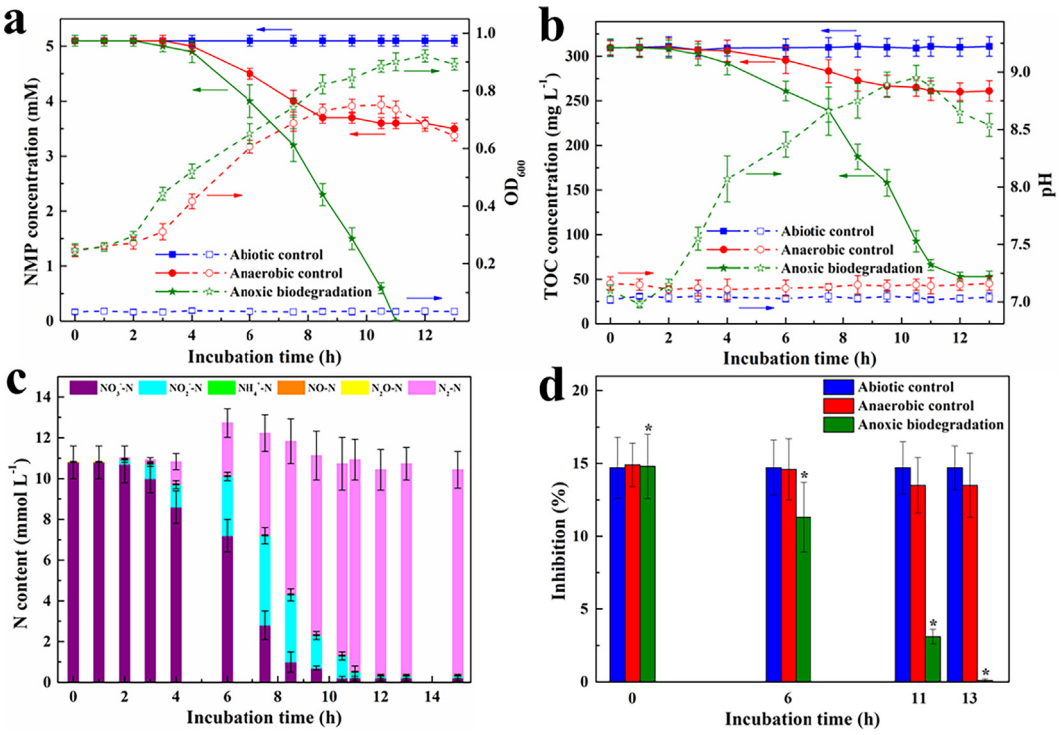

Fig. 1. NMP biodegradation performance: (a) NMP biodegradation and cell growth; (b) TOC removal and pH variation; (c) N content; (d) toxicity reduction.

6.0 h, providing key evidence for the conversion of nitrogen in NMP into inorganic-N (Fig. 1c). Considering the increase of OD_{600} value, nitrogen in NMP might be served as nutrient substance for cell growth during NMP biodegradation process. It was quite interesting that pH in NMP biodegradation system supplemented with nitrate increased obviously from initial 7.1 ± 0.1 to 8.9 ± 0.2 after 9.5 h, confirming the occurrence of denitrification (Qian et al., 2019).

Toxicity reduction during NMP biodegradation by NJUST38 was evaluated using luminescence inhibition toxicity profile (Xu et al., 2018). As illustrated in Fig. 1d, the initial inhibition ratio of the influent containing 5 mM NMP was calculated as 14.7 ± 2.1%. The inhibition ratio obviously decreased to 11.3 ± 2.4% and 3.1 ± 0.5% after 6 h and 11 h, respectively, accompanied by NMP biodegradation under anoxic conditions with the supplementation of 10.8 mM nitrate. The inhibition ratio further decreased to 0.1 ± 0.1% at 13.0 h, indicating the almost complete removal of toxicity by NJUST38. Nevertheless, the inhibition ratio only slightly decreased to 13.5 ± 2.2% in the control anaerobic system even after 13-h incubation. The inhibition ratio in the abiotic control system maintained a constant value during the entire incubation period, which was consistent with NMP concentration profile.

EEM analysis was performed to reveal variations in dissolved organic matter (DOM) during NMP biodegradation process. As indicated in Fig. 2a, the most apparent fluorophores for the influent containing 5.0 mM NMP was observed at excitation/emission wavelengths (Ex/Em) of 230 nm/325–340 nm in region I and region II, and 280 nm/328–340 nm in region IV. No obvious variations were observed for the fluorophores in regions I, II or IV for the abiotic control system after incubation for 11 h (Fig. 2b). The intensity of fluorophores decreased slightly in the control anaerobic system without nitrate (Fig. 2c), which was consistent with the slight decrease in NMP concentration. Notably, the intensity of fluorophores in regions I, II and IV decreased significantly in the effluent from the anoxic system compared to the influent, indicating the remarkably enhanced removal of DOM (Fig. 2d). EEM analyses were consistent with the NMP concentration profiles and confirmed the efficient biotransformation of NMP in the anoxic system.

3.2. Probable products and pathway for NMP biodegradation

During NMP anoxic biodegradation by NJUST38, several intermediates identified through HPLC and HPLC/MS are shown in Supplementary data. The peak of NMP appeared at retention time of 2.77 min (m/z = 121 $[M + Na]^+$). After incubation in the anoxic system assisted with nitrate for 11 h, a new biodegradation intermediate (M1) was observed at retention time of 1.80 min with m/z of 115.60 $[M\text{-}H]^-$. The mass of 115.60 $[M\text{-}H]^-$ indicated that it could be tentatively assigned as a single hydrolytic product of NMP namely N-methylaminobutyric acid (M1). According to Solis-Gonzalez et al. (2018), the hydrolysis reaction commonly occurred at the acylamino group of NMP. The peak with m/z of 100.75 $[M\text{-}H]^-$ (M2), which showed high signal intensity, could be tentatively speculated to be the oxidation product of M1 namely succinic semialdehyde, since succinic semialdehyde was reported as the intermediate during NMP biodegradation (Cai et al., 2014; Solis-Gonzalez et al. 2018). NMP biodegradation intermediates by NJUST38 under anaerobic condition showed low signal intensity of M2 and high signal intensity of M1, indicating that NMP could be degraded feebly through hydrolysis in anaerobic system without nitrate.

Based on the identified products, the possible pathway for NMP biodegradation in anoxic system was proposed as follows: apparently, hydrolysis of NMP might be the initial step regardless of presence or absence of nitrate, and N-methylaminobutyric acid (M1) was expected to be the direct product arose from this hydrolysis. Subsequently, N-methylaminobutyric acid was transformed into succinate semialdehyde (M2) through deamination, which was then oxidized to succinate to entry into TCA cycle. This could be supported by previous studies, where hydrolysis, deamination and oxidation were considered as the main biotransformation reactions for NMP biodegradation by pure culture (Cai et al., 2014; Solis-Gonzalez et al. 2018). To further verify NMP biodegradation pathway proposed above, the genome information of strain NJUST38 and gene expression level relative to microbial metabolism between anoxic and anaerobic systems were analyzed.

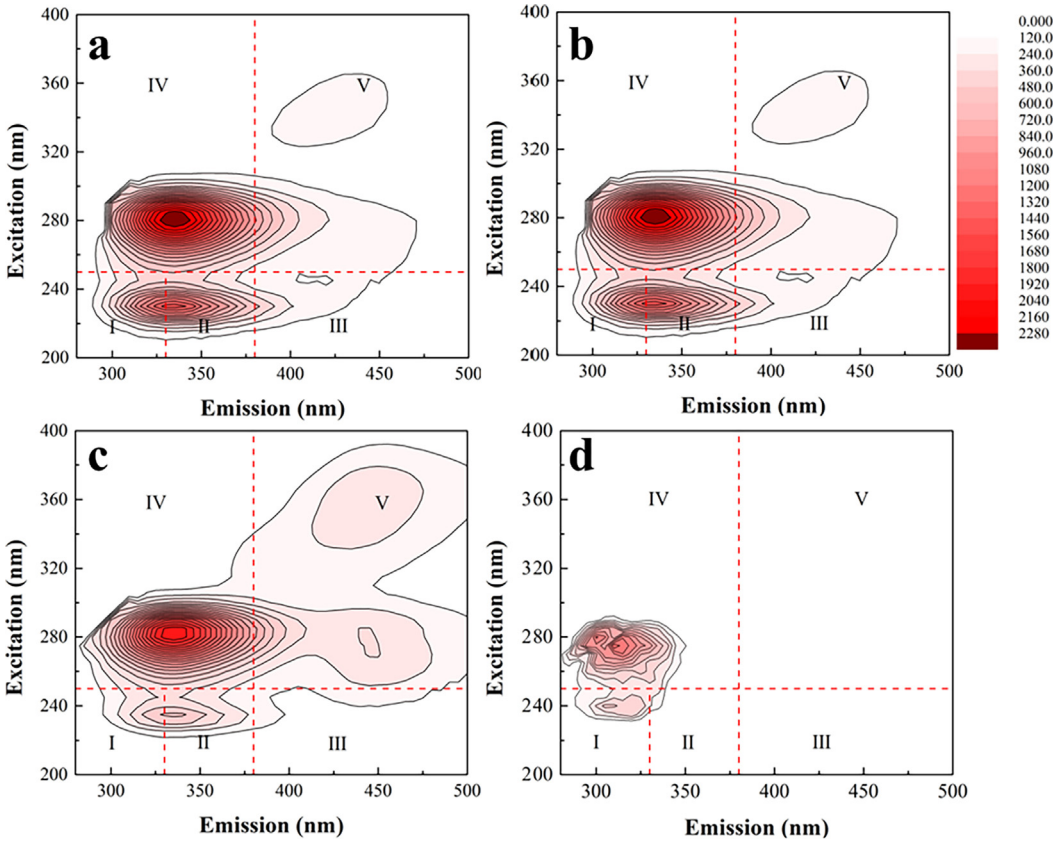

Fig. 2. EEM analysis: (a) influent; (b) effluent from abiotic control system; (c) effluent from anaerobic control system; (d) effluent from anoxic system.

3.3. Genomic characterization and transcriptomic analysis

Genomic information of NJUST38 was revealed to obtain clear insight into bacterial metabolism mechanisms (Fig. 3a). The size of the genome was 4.25 Mbp in total, with an average GC content of 67.84%. The chromosome of the NJUST38 genome contained 4188 open-reading frames (ORFs), of which 3713 (88.87%) were identified as putative coding sequences (CDS). A group of 48 RNA genes, including single copy of sRNA, 5S, 16S and 23S rRNA genes, were found in these CDS. A COG-based analysis results showed that 464 (12%), 242 (6%), 210 (5%) and 143 (4%) of the COG functions were responsible for transport and metabolism of amino acids, carbohydrate and lipid compounds as well as biosynthesis and catabolism of secondary metabolites, respectively. In addition, the KEGG functional annotation indicated that NJUST38 could metabolize a variety of xenobiotics, nucleotides and glycan compounds. The whole-genome sequences were deposited at DDBJ/ENA/GenBank (WGS: accession number RIAQ00000000, version RIAQ01000000; SRA: accession number SRR8346068).

In order to explore the effect of nitrate stimulation on NMP metabolism, the genome-wide transcriptional profiling of NJUST38 with nitrate or without nitrate was investigated. The RNA-Seq toolset was used for quantifying expression levels of transcripts and identifying the potential molecular mechanisms responsible for microbial metabolism. The total number of bases from six samples was greater than 14.60 GB, and the Q30 percentage was over 95%. The average GC content was greater than 66.43%. By comparing with anaerobic system (Aa1 group), a total of 561 (Ao1 group) and 1603 (Ao2 group) differential expressed genes (DGEs) were obtained from anoxic system, of which 141 (Ao1) and 725 (Ao2) genes were up-regulated at the presence of nitrate, as shown in Supplementary data. These DGEs were subsequently used for functional annotation and enrichment analysis by GO classification and KEGG annotations to allow normalized comparisons between anoxic and anaerobic systems. GO enrichments revealed that the molecular function category with the greatest abundance was electron transfer activity. The DGEs were subjected to KEGG pathways in order to gain additional information about the potential involvement of specific metabolic pathways in the regulation of microbial metabolism (Fig. 3b). Analysis of the top 20 KEGG pathways showed that metabolic pathways, microbial metabolism in diverse environments, nitrogen metabolism, biosynthesis of secondary metabolites and carbon metabolism, were significantly enrichment in anoxic groups, such as RNA polymerase subunit beta (*rpoC*, gene id: L633_RS0119440) mainly responsible for cell growth, indicating more rapid bacterial growth in the anoxic system, which was consistent with the variation of OD_{600} value (Richardson et al., 2012). Therefore, the addition of nitrate was able to cause substantial stimulation on cellular regulation and microbial metabolism.

3.4. Highly expressed genes involved in NMP biodegradation and denitrification

Previous studies confirmed that microbial denitrification was often accomplished in intracellularly by a series of biological reactions, which were commonly driven by a series of electron transports and consumptions (Wan et al., 2016). Denitrification was primarily catalyzed by four essential denitrifying enzymes, namely, nitrate reductase (NAR), nitrite reductase (NIR), nitric oxide reductase (NOR) and nitrous oxide reductase (N_2OR), respectively (Su et al., 2019). Fig. 4a displays the gene expressions of these denitrifying enzymes, i.e., *narGHJI* (encoding nitrate reductase), *nirS* (encoding nitrite reductase), *norBC* (encoding nitric oxide reductase) and *nosZ* (encoding nitrous oxide reductase), were significantly up-regulated in anoxic system compared to anaerobic system without nitrate. It can be found that the up-regulated log2.FoldChange for *narG*, *narH*, *narJ*, *narI*, *nirS*, *norB*, *norC* and *nosZ* were 4.8, 5.0, 4.5, 5.2, 3.1, 5.6, 5.1 and 3.1, respectively (Fig. 4b).

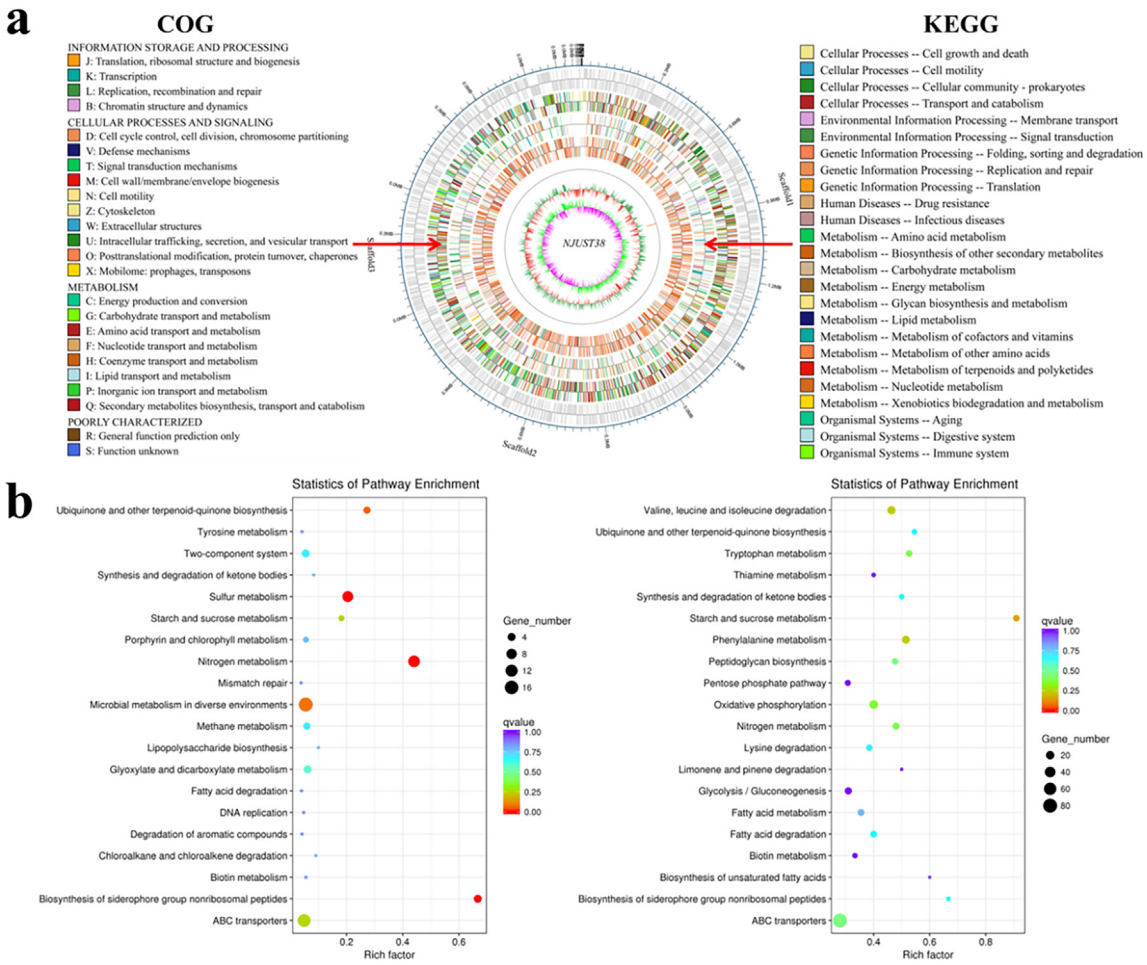

Fig. 3. (a) Genomic characterization of NJUST38 with gene function annotations (COG & KEGG) and (b) KEGG pathways annotation of the differentially expressed genes in the anoxic system.

Moreover, gene *nrt*, which was responsible for nitrate/nitrite transport, was observed significantly up-regulated with log2.FoldChange of 3.9. Clearly, over expression of these denitrifying enzymes/genes require greater reducing power and electrons supply, which might be the most important reason for enhanced NMP biodegradation.

NMP biodegradation provides electrons to support denitrification, while NMP can be catabolized via a well-established pathway (Sadauskas et al., 2017). Mao et al. (2014) demonstrated that *Candidatus* could utilize the TCA cycle to provide electron and reducing power for microbial metabolism. Similar to indole (Solis-Gonzalez et al. 2018; Sadauskas et al., 2017), NMP metabolites could reach TCA cycle to counteract the toxic effects of NMP and its derivatives. The presence of succinate dehydrogenase (*sdh*), fumarate reductase (*frd*), malate dehydrogenase (*maeB*), succinyl-CoA synthetase (*sucCD*) and isocitrate dehydrogenase (*icd*) suggested the scenario of TCA cycle in NJUST38 (Supplementary data). The significant enhancement of TCA cycle in anoxic system further demonstrated that both electron transport efficiency and energy metabolism could be improved at the presence of nitrate.

To identify potential genes associated with NMP metabolism, we analyzed the transcriptional levels of keys genes related to NMP biodegradation in both anoxic and anaerobic systems. Similar to *Alicycliphilus* (Solis-Gonzalez et al. 2018), key genes were implicated in NMP metabolism, i.e., N-methylhydantoin amidohydrolase (*hyuB*), which activated hydrolysis and N-heterocyclic cleavage of NMP at the beginning of biodegradation; Methyltransferase (*cobA*), which was responsible for demethylation; 4-aminobutyrate-2-oxoglutarate transaminase (*gabT*), which activated deamination; succinate-semialdehyde dehydrogenase (*gabD*), which activated the transformation of succinate-semialdehyde to succinate. It could be found that gene expression of *hyuB* (log2.FoldChange = 2.0) and *cobA* (log2.FoldChange = 4.3), could be significantly up-regulated with the addition of nitrate, which might be an important reason for the enhanced NMP biodegradation. Gene *cobA* might be catalyzing the demethylation and methanol production simultaneously (Warren et al., 1990; Geng et al., 2018). Importantly, the key genes related to methanol metabolism, including alcohol dehydrogenase (*adhP*, log2.FoldChange = 4.5), aldehyde dehydrogenase (*aldB*, log2.FoldChange = 3.3) and formate dehydrogenase subunit alpha (*fdhA*, log2.FoldChange = 4.5), were detected significantly up-regulated under anoxic condition, which was consistent with the high expression of *cobA*. Hence, the electron production could be accelerated at the presence of nitrate to complete denitrification, resulting in positive effect on intracellular metabolism of NMP.

3.5. Mechanism dominating NMP biodegradation and denitrification

A scheme for NMP biodegradation and denitrification in NJUST38 was proposed based on the above analysis. First, microbial denitrification starts with NO_3^- reduction to NO_2^-, and this reduction requires electrons and reducing power (Fig. 5a). NMP is biologically activated via N-methylhydantoin amidohydrolase (*hyuB*), Methyltransferase (*cobA*), 4-aminobutyrate-2-oxoglutarate transaminase (*gabT*), succinate-semialdehyde dehydrogenase (*gabD*), and so on (Fig. 5b & 5c). Notably, the generation of intermediates, such as N-methylaminobutyric acid, was catalyzed by *hyuB*, which activated the hydrolysis of acylamino on NMP. Generation of intermediates including

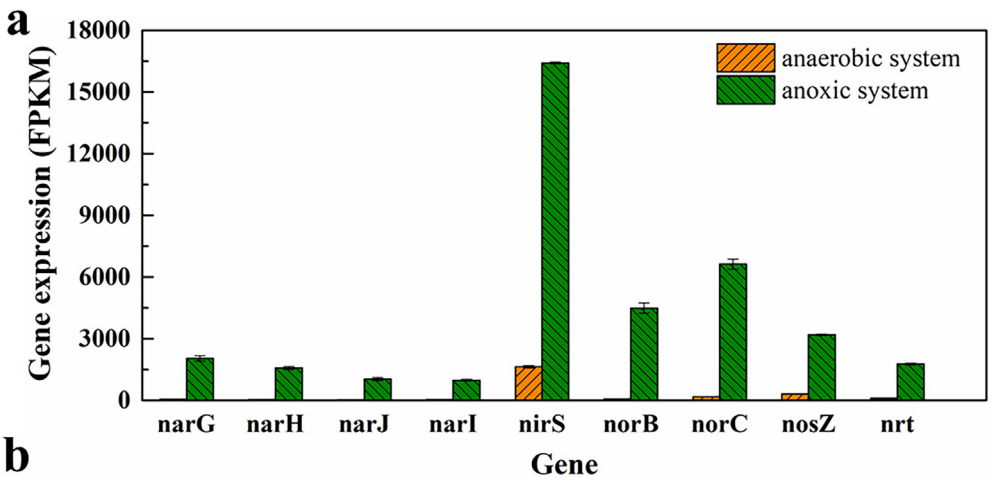

Gene	Gene description	Gene_id	Length (nt)	log2.FoldChange
narG	nitrate reductase subunit alpha	L633_RS0101885	3765	4.8052
narH	nitrate reductase subunit beta	L633_RS0101880	1518	4.9694
narJ	nitrate reductase	L633_RS0101875	690	5.1714
narI	nitrate reductase subunit gamma	L633_RS0101870	702	4.5460
nirS	nitrite reductase	L633_RS0104450	1791	3.0912
norB	nitric oxide reductase	L633_RS0104470	1389	5.6472
norC	nitric oxide reductase subunit C	L633_RS0104465	453	5.0612
nosZ	nitrous-oxide reductase	L633_RS0101800	1959	3.1443
nrt	nitrate/nitrite transporter	L633_RS0101890	2718	3.8865

Fig. 4. Key enzymes/genes involved in microbial denitrification in strain NJUST38: (a) gene expression dynamic between anaerobic and anoxic systems; (b) gene length and log2.FoldChange of functional genes involved in denitrification.

aminobutyric acid and succinate-semialdehyde, was catalyzed by *cobA* and *gabT*, respectively. The intermediate namely methanol could be further degraded, which was catalyzed by alcohol, aldehyde and formate dehydrogenases (*adhP*, *aldB*, *fdhA*). The intermediate succinate-semialdehyde could be further oxidized to succinate to reach TCA cycle for supporting denitrification.

Electron transport and consumption are quite essential for these sequential interactions, including NMP biodegradation and denitrification (Wan et al., 2016), because the electrons and reduction power required for denitrification are generated simultaneously via NMP biodegradation. Electrons were fed into the quinone pool via key proteins encoding electron transport pathway, such as succinate dehydrogenases and flavoproteins. Cytochrome c1 relays electrons from the quinone pool inside the membrane to the cytochrome *c*, which was then consumed by terminal reductases, such as NIR, NOR and N_2OR (Wan et al., 2016; Barnard et al., 2004). Electrons are delivered from NADH via NADH dehydrogenase, quinone pool, succinic dehydrogenase, cytochrome *b*, cytochrome c1 and cytochrome *c* before consumption in the reductive reaction catalyzed by NAR, NIR, NOR and N_2OR (Wan et al., 2016). Gene expression of key electron transport proteins, including succinate dehydrogenase, cytochrome *b*, cytochrome c1 and cytochrome *c*, were significantly up-regulated at the presence of nitrate, resulting in higher electron transport efficiency, as indicated in Supplementary data. The sequential reduction of NO_3^- to NO_2^-, NO and N_2O requires abundant electrons supply, providing a continuous sink for the electrons from NMP biodegradation and/or TCA cycle (Mao et al., 2014). It is rather crucial for enhancing NMP biodegradation through the improvement of electron transport efficiency and activity.

3.6. Key enzymes, NADH and electron transport system activity

The activity of key enzymes related to NMP biodegradation, denitrification and electron transport system (ETS) as well as NADH (the direct electron donor for denitrification) content, was further determined in this study. The corresponding enzymatic activities, including N-methylhydantoin amidohydrolase (NMA), NAR, NIR, NOR and N_2OR as well as ETS, were set as 100% in the anaerobic system without nitrate to compare differences between anaerobic and anoxic condition.

Previous studies showed that hydrolase was an important enzyme for the breakdown of C–C/C-N bonds during N-heterocyclic compounds degradation (Jia et al., 2018; Yu et al., 2019). During NMP biodegradation process, the activity of NMA, which catalyzed the conversion of NMP to N-methylaminobutyric acid, was remarkably enhanced by 64.5 ± 10.1% ($p < 0.05$) under anoxic condition compared with anaerobic condition (Fig. 6a). Concentration of the electron carrier (NADH) was thus increased (Fig. 6b), which was well match with the higher gene expression of N-methylhydantoin amidohydrolase (*hyuB*). On average, NADH content under anoxic condition was 69.1 ± 5.9% ($p < 0.05$) higher than anaerobic condition.

ETS activity assay indicated that the microbial ETS activity in the anoxic system was significantly increased by 87.3 ± 17.5% ($p < 0.05$) compared with anaerobic system without nitrate (Fig. 6a), which was consistent with the gene expression profile. After transport, the electrons were mainly consumed by four key denitrifying enzymes, i.e., NAR, NIR, NOR and N_2OR. The enzymatic activity assays revealed that the activity of NAR, NIR, NOR and N_2OR was increased by 46.8 ± 8.5%, 64.1 ± 21.3%, 85.4 ± 10.7% and 60.9 ± 12.1% in anoxic system compared with anaerobic control system (Fig. 6a). Clearly, the presence of nitrate enhanced electrons production, transport and consumption, thereby increased electron supplying capacity, and simultaneously enhanced NMP biodegradation.

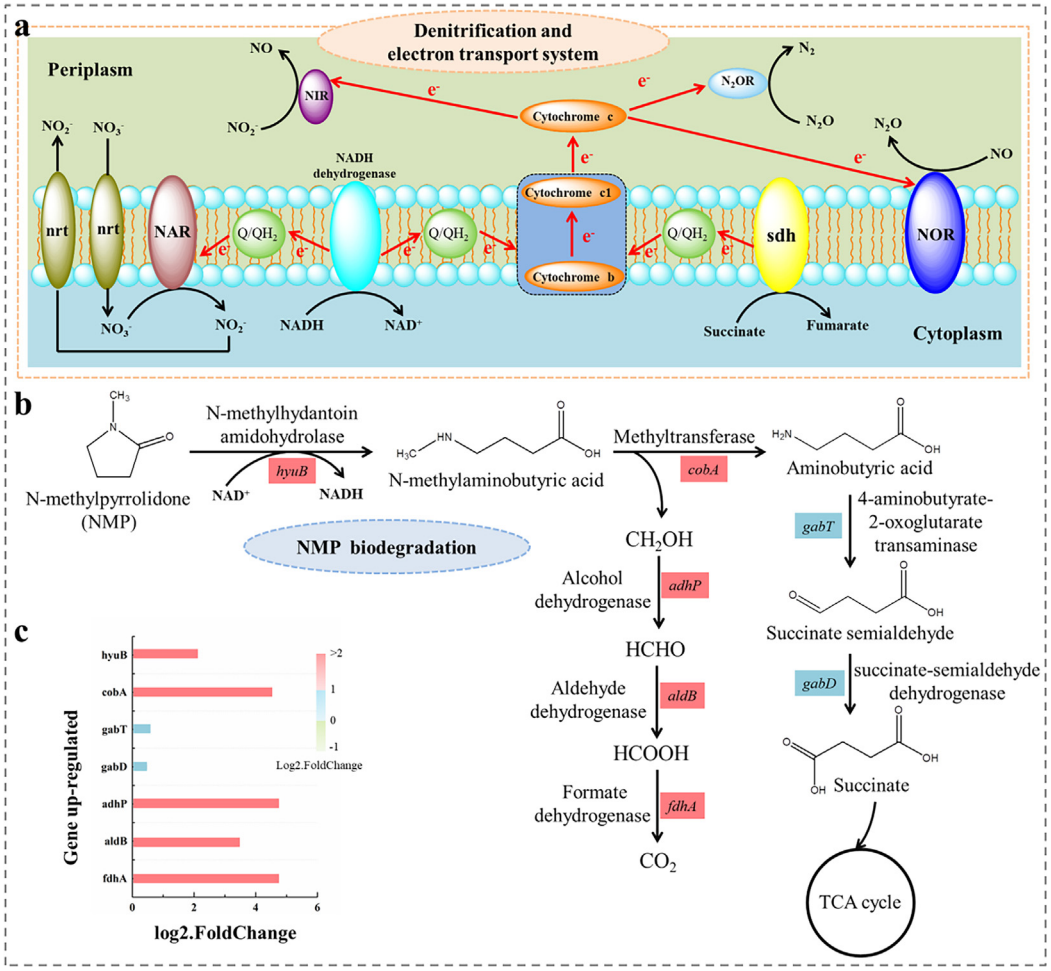

Fig. 5. Mechanism involved in NMP biodegradation, denitrification and electron transport in the anoxic system: (a) microbial denitrification and electron transport system in NJUST38, Q/QH_2 represented quinone pool; (b) NMP biodegradation mechanism; (c) up-regulated genes dominating NMP biodegradation, red color represented significantly up-regulated gene, blue color represented mildly up-regulated gene. (For interpretation of the references to color in this figure legend, the reader is referred to the web version of this article.)

4. Conclusion

In this study, a novel strain namely *Paracoccus pantotrophus* NJUST38, which was capable of biodegrading NMP under anoxic conditions, was firstly isolated and identified. NJUST38 was highly efficient on NMP biodegradation, toxicity reduction and TOC removal in anoxic system with the supplementary of electron acceptor, i.e., nitrate. The sequential reductions of NO_3^- to N_2 providing a continuous "reception sink" for electrons from NMP biodegradation and/or TCA cycle, which was responsible for enhanced NMP biodegradation. NMP metabolic mechanism provides new insights into the environmental fate and potential ecological impact of NMP.

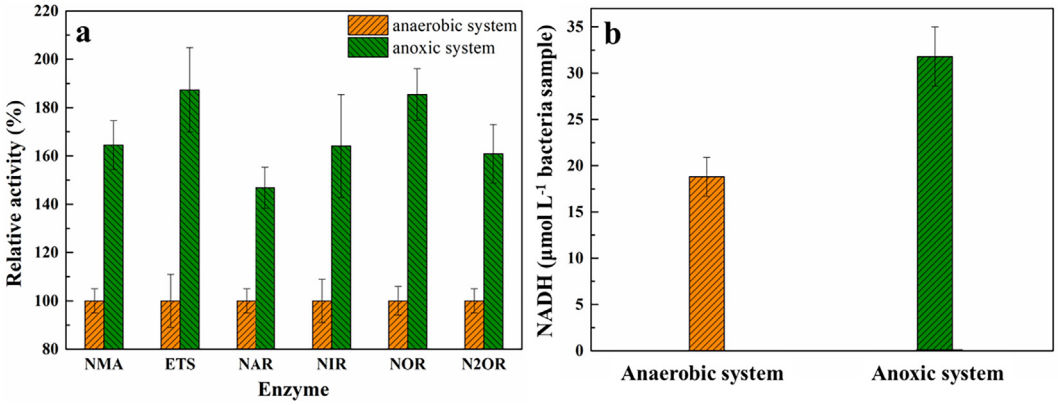

Fig. 6. The relative activities of key enzymes, ETS and NADH content involved in NMP biodegradation and denitrification: (a) Relative activities of NMA, ETS, NAR, NIR, NOR and N_2OR in both anaerobic and anoxic systems; (b) NADH content in both anaerobic and anoxic systems.

Declaration of Competing Interest

The authors declare that they have no known competing financial interests or personal relationships that could have appeared to influence the work reported in this paper.

Acknowledgments

This research is financed by Natural Science Foundation of Jiangsu Province (BK20170038) and National Natural Science Foundation of China (No. 51922050).

Appendix A. Supplementary data

Supplementary data to this article can be found online at https://doi.org/10.1016/j.biortech.2019.122185.

References

Barnard, R., Barthes, L., Le Roux, X., Leadley, P.W., 2004. Dynamics of nitrifying activities, denitrifying activities and nitrogen in grassland mesocosms as altered by elevated CO_2. New Phytol. 162, 365–376.

Cai, S., Cai, T.M., Liu, S.Y., Yang, Q., He, J., Chen, L.W., Hu, J., 2014. Biodegradation of N-methylpyrrolidone by *Paracoccus* sp. NMD-4 and its degradation pathway. Int. Biodeter. Biodegr. 93, 70–77.

Campbell, H.L., Striebig, B.A., 1999. Evaluation of N-methylpyrrolidone and its oxidative products toxicity utilizing the microtox assay. Environ. Sci. Technol. 33, 1926–1930.

Carvajal, A., Akmirza, I., Navia, D., Perez, R., Munoz, R., Lebrero, R., 2018. Anoxic denitrification of BTEX: Biodegradation kinetics and pollutant interactions. J. Environ. Manage. 214, 125–136.

Chen, D., Shen, J.Y., Jiang, X.B., Su, G.Y., Han, W.Q., Sun, X.Y., Li, J.S., Mu, Y., Wang, L.J., 2019a. Simultaneous debromination and mineralization of bromophenol in an up-flow electricity-stimulated anaerobic system. Water Res. 157, 8–18.

Chen, Y., Su, X.X., Wang, Y.Y., Zhao, S.Y., He, Q., 2019b. Short-term responses of denitrification to chlorothalonil in riparian sediments: Process, mechanism and implication. Chem. Eng. J. 358, 1390–1398.

Geng, C., Zhao, T.F., Yang, C.X., Zhang, Q.Z., Bai, F., Zeng, J.L., Zhang, F.Y., Liu, X.Q., Lan, X.Z., Chen, M., Liao, Z.H., 2018. Metabolic characterization of *Hyoscyamus niger* root-specific putrescine *N*-methyltransferase. Plant Physiol. Bioch. 127, 47–54.

Hou, C., Shen, J.Y., Jiang, X.B., Zhang, D.J., Sun, X.Y., Li, J.S., Han, W.Q., Liu, X.D., Wang, L.J., 2018. Enhanced anoxic biodegradation of pyridine coupled to nitrification in an inner loop anoxic/oxic-dynamic membrane bioreactor (A/O-DMBR). Bioresour. Technol. 267, 626–633.

Jia, Y.Y., Khanal, S.K., Shu, H.Y., Zhang, H.Q., Chen, G.H., Lu, H., 2018. Ciprofloxacin degradation in anaerobic sulfate-reducing bacteria (SRB) sludge system: Mechanism and pathways. Water Res. 136, 64–74.

Jiang, X.B., Shen, J.Y., Xu, K.C., Chen, D., Mu, Y., Sun, X.Y., Han, W.Q., Li, J.S., Wang, L.J., 2018. Substantial enhancement of anaerobic pyridine bio-mineralization by electrical stimulation. Water Res. 130, 291–299.

Krizek, K., Ruzicka, J., Julinova, M., Husarova, L., Houser, J., Dvorackova, M., Jancova, P., 2015. N-methyl-2-pyrrolidone-degrading bacteria from activated Sludge. Water Sci. Technol. 71, 776–782.

Lee, J.J., Rhee, S.K., Lee, S.T., 2001. Degradation of 3-methylpyridine and 3-ethylpyridine by *Gordonia nitida* LE31. Appl. Environ. Microbiol. 67, 4342–4345.

Li, H.X., Zhou, L.J., Lin, H., Xu, X.Y., Jia, R.Y., Xia, S.Q., 2018. Dynamic response of biofilm microbial ecology to para-chloronitrobenzene biodegradation in a hydrogen-based, denitrifying and sulfate-reducing membrane biofilm reactor. Sci. Total. Environ. 643, 842–849.

Li, P., Wang, Y.J., Zuo, J.E., Wang, R., Zhao, J., Du, Y.J., 2017. Nitrogen removal and N_2O accumulation during hydrogenotrophic denitrification: influence of environmental factors and microbial community characteristics. Environ. Sci. Technol. 51, 870–879.

Liang, X.J., Ye, S.L., Xie, Q.L., Lu, M.Z., Xia, F., Nie, Y., Pan, Z.Y., Ji, J.B., 2018. Solubilities of sulfuryl fluoride in propylene carbonate, tributyl phosphate and N-methylpyrrolidone. J. Chem. Thermodynamics 125, 11–16.

Loh, C.H., Wu, B., Ge, L.Y., Pan, C.Z., Wang, R., 2018. High-strength N-methyl-2-pyrrolidone-containing process wastewater treatment using sequencing batch reactor and membrane bioreactor: A feasibility study. Chemosphere 194, 534–542.

Mahdavianpour, M., Moussavi, G., Farrokhi, M., 2018. Biodegradation and COD removal of *p*-Cresol in a denitrification baffled reactor: Performance evaluation and microbial community. Process Biochem. 69, 153–160.

Mao, Y.P., Yu, K., Xia, Y., Chao, Y.Q., Zhang, T., 2014. Genome reconstruction and gene expression of "*Candidatus* Accumulibacter phosphatis" clade IB performing biological phosphorus removal. Environ. Sci. Technol. 48, 10363–10371.

Qian, W.T., Ma, B., Li, X.Y., Zhang, Q., Peng, Y.Z., 2019. Long-term effect of pH on denitrification: High pH benefits achieving partial-denitrification. Bioresour. Technol. 278, 444–449.

Ren, Q.Q., Zhao, C.S., Duan, L.B., Chen, X.P., 2011. NO formation during agricultural straw combustion. Bioresour. Technol. 102, 7211–7217.

Richardson, L.A., Reed, B.J., Charette, J.M., Freed, E.F., Fredrickson, E.K., Locke, M.N., Baserga, S.J., Gardner, R.G., 2012. A conserved deubiquitinating enzyme controls cell growth by regulating RNA polymerase I stability. Cell Rep. 2, 372–385.

Sadauskas, M., Vaitekunas, J., Gasparaviciute, R., Meskys, R., 2017. Indole biodegradation in *Acinetobacter* sp. Strain O153: genetic and biochemical characterization. Appl. Environ. Microb. 83, e01453–e1517.

Shen, J.Y., Chen, Y., Wu, S.J., Wu, H.B., Liu, X.D., Sun, X.Y., Li, J.S., Wang, L.J., 2015. Enhanced pyridine biodegradation under anoxic condition: The key role of nitrate as the electron acceptor. Chem. Eng. J. 277, 140–149.

Solis-Gonzalez, C.J., Dominguez-Malfavon, L., Vargas-Suarez, M., Gaytan, I., Cevallos, M.A., Lozano, L., Cruz-Gomez, M.J., Loza-Tavera, H., 2018. Novel metabolic pathway for N-methylpyrrolidone degradation in *Alicycliphilus* sp. strain BQ1. Appl. Environ. Microb. 84, e02136–e2217.

Su, X.X., Chen, Y., Wang, Y.Y., Yang, X.Y., He, Q., 2019. Impacts of chlorothalonil on denitrification and N_2O emission in riparian sediments: Microbial metabolism mechanism. Water Res. 148, 188–197.

Tian, T., Qiao, S., Yu, C., Tian, Y.H., Yang, Y., Zhou, J.T., 2017. Distinct and diverse anaerobic respiration of methanogenic community in response to MnO_2 nanoparticles in anaerobic digester sludge. Water Res. 123, 206–215.

Wan, R., Chen, Y.G., Zheng, X., Su, Y.L., Li, M., 2016. Effect of CO_2 on microbial denitrification via inhibiting electron transport and consumption. Environ. Sci. Technol. 50, 9915–9922.

Wang, J., Jiang, X.B., Liu, X.D., Sun, X.Y., Han, W.Q., Li, J.S., Wang, L.J., Shen, J.Y., 2018a. Microbial degradation mechanism of pyridine by *Paracoccus* sp. NJUST30 newly isolated from aerobic granules. Chem. Eng. J. 344, 86–94.

Wang, L., Liu, Y.L., Wang, C., Zhao, X.D., Mahadeva, G.D., Wu, Y.C., Ma, J., Zhao, F., 2018b. Anoxic biodegradation of triclosan and the removal of its antimicrobial effect in microbial fuel cells. J. Hazard. Mater. 344, 669–678.

Wang, X., Zhang, M., Liu, J., Zhang, G., Yang, J., 2010. Thermal degradation of poly (arylene sulfide sulfone)/nemthylpyrrolidone carystal solvate. Chinese J. Polym. Sci. 28, 85–91.

Wang, Y., Zhang, X.F., Yang, S.L., Yuan, Y.B., 2018c. Lignin involvement in programmed changes in peach-fruit texture indicated by metabolite and transcriptome analyses. J. Agric. Food Chem. 66, 12627–12640.

Warren, M.J., Gonzalez, M.D., Williams, H.J., Stolowich, N.J., Scott, A.I., 1990. Uroporphyrinogen-III methylase catalyzes the enzymatic-synthesis of sirohydrochlorin-II and sirohydrochlorin-IV by a clockwise mechanism. J. Am. Chem. Soc. 112, 5343–5345.

Wu, H.B., Sun, Q.Q., Sun, Y.L., Zhou, Y.K., Wang, J., Hou, C., Jiang, X.B., Liu, X.D., Shen, J.Y., 2019. Co-metabolic enhancement of 1H–1,2,4-triazole biodegradation through nitrification. Bioresour. Technol. 271, 236–243.

Wu, H.B., Shen, J.Y., Jiang, X.B., Liu, X.D., Sun, X.Y., Li, J.S., Han, W.Q., Mu, Y., Wang, L.J., 2018. Bioaugmentation potential of a newly isolated strain *Sphingomonas* sp. NJUST37 for the treatment of wastewater containing highly toxic and recalcitrant tricyclazole. Bioresour. Technol. 264, 98–105.

Xu, Y.Q., Liu, S.S., Fan, Y., Li, K., 2018. Toxicological interaction of multi-component mixtures to *Vibrio qinghaiensis* sp.-Q67 induced by at least three components. Sci. Total. Environ. 635, 432–442.

Yan, Z.S., He, Y.H., Cai, H.Y., Van Nostrand, J.D., He, Z.L., Zhou, J.Z., Krumholz, L.R., Jiang, H.L., 2017. Interconnection of key microbial functional genes for enhanced Benzo[a]pyrene biodegradation in sediments by microbial electrochemistry. Environ. Sci. Technol. 51, 8519–8529.

Yau, H.C., Bayazit, M.K., Steinke, J.H.G., Shaffer, M.S.P., 2015. Sonochemical degradation of N-methylpyrrolidone and its influence on single walled carbon nanotube dispersion. Chem. Commun. 51, 16621–16624.

Young Young, M.D., Wakefield, M.J., Smyth, G.K., Oshlack, A., 2010. Gene ontology analysis for RNA-seq: accounting for selection bias. Genome Biol. 11 R14-R14.

Yu, K., Yi, S., Li, B., Guo, F., Peng, X.X., Wang, Z.P., Wu, Y., Alvarez-Cohen, L., Zhang, T., 2019. An integrated meta-omics approach reveals substrates involved in synergistic interactions in a bisphenol A (BPA)-degrading microbial community. Microbiome 7, 16.

Yun, H., Liang, B., Kong, D.Y., Cheng, H.Y., Li, Z.L., Gu, Y.B., Yin, H.Q., Wang, A.J., 2017. Polarity inversion of bioanode for biocathodic reduction of aromatic pollutants. J. Hazard. Mater. 331, 280–288.

Zhang, T., Huang, Z., Chen, X.H., Huang, M.Z., Ruan, J.J., 2016. Degradation behavior of dimethyl phthalate in an anaerobic/anoxic/oxic system. J. Environ. Manage. 184, 281–288.

Zhao, B., An, Q., He, Y.L., Guo, J.S., 2012. N2O and N2 production during heterotrophic nitrification by Alcaligenes faecalis strain NR. Bioresour. Technol. 116, 379–385.

Zolfaghari, A., Mortaheb, H.R., Meshkini, F., 2011. Removal of N-methyl-2-pyrrolidone by photocatalytic degradation in a batch reactor. Ind. Eng. Chem. Res. 50, 9569–9576.